

## ORIGINAL ARTICLE

# Elastogenic potential and antisagging properties of a novel *Murraya koenigii* extract

Chloé Lorion PhD  | Viviane Bardin | Sébastien Bonnet | Amandine Lopez-Gaydon | Boris Vogelgesang | Nicolas Bechetoille PhD 

Gattefossé SAS, Saint-Priest Cedex,  
France

**Correspondence**

Chloé Lorion, Gattefossé SAS, R&D, 36  
chemin de Genas, CS 70070, 69804 Saint-  
Priest Cedex, France.

Email: [clorion@gattefosse.com](mailto:clorion@gattefosse.com)

**Abstract**

**Background:** The process by which functional elastic fibers are produced, namely elastogenesis, is complex and difficult to assess in vitro. Identifying efficient elasticity-boosting ingredients thus represents a challenge.

**Aims:** The elasticity-boosting properties of a novel extract of *Murraya koenigii* leafy stems were assessed in vitro in 3D culture models before being evaluated in human female volunteers.

**Methods:** Synthesis of elastic fiber related proteins was evaluated in a skin-equivalent model. Using multiphoton microscopy, the structural organization of elastin deposits was studied within a scaffold-free dermal microtissue. Biomechanical properties of the 3D microtissue were also measured by atomic force microscopy. In vivo, fringe-projection and image analysis were used to evaluate nasogenian fold severity in a panel of Caucasian female volunteers. The impact of gravity on visible signs of facial aging was assessed by clinical scoring carried out alternatively in the supine and sitting positions.

**Results:** We showed the *Murraya koenigii* extract increased protein expressions of elastin and fibrillin-1 in a 3D skin equivalent model. Using scaffold-free dermal microtissue, we confirmed that *Murraya koenigii* extract allowed a proper and ordered network of elastin deposits and consequently improved tissue elasticity. Clinical data showed that a twice-daily application for 98 days of the extract formulated at 1% allowed to visibly reduce nasogenian fold severity, jowl severity and to mitigate the impact of gravity on the facial signs of aging.

**Conclusion:** The newly discovered extract of *Murraya koenigii* leafy stems represents an innovative antiaging ingredient suited for elasticity-boosting and antisagging claims.

**KEYWORDS**

3D models, elastic fibers, *Murraya koenigii* extract, skin aging, skin sagging

This is an open access article under the terms of the [Creative Commons Attribution](https://creativecommons.org/licenses/by/4.0/) License, which permits use, distribution and reproduction in any medium, provided the original work is properly cited.

© 2023 Gattefossé SAS. *Journal of Cosmetic Dermatology* published by Wiley Periodicals LLC.

## 1 | INTRODUCTION

Human skin offers a mechanical barrier against environmental damage thanks to the reversible deformation of its structure. More particularly, the dermal extracellular matrix (ECM) ensures an essential role in skin cohesion and strongly influences biomechanical properties. Within the ECM, elastic fibers represent the primary effectors of skin elasticity and resilience. Indeed, elastin allows for a reversible deformation and recoil, with an ability to extend several times beyond its resting length and reversibly return to its original state.<sup>1</sup> Elastic fibers form a complex network still only partially understood. The properly organized arrangement of the elastic fiber network is more important than the abundance of fibers per se, as regards their functionality and resulting biomechanical properties. Elastin constitutes the central core of elastic fibers, surrounded by a microfibril sheath rich in fibrillin-1, the most abundant fibrillin isoform in the adult dermis.<sup>2</sup> Besides, a wide array of fibrillin-associated proteins is known to facilitate the assembly of elastic fibers and contribute to their functionality. Among them, fibulin-5 is essential to elastic fiber development. Indeed, localized at the surface of elastic fibers, fibulin-5 contributes to elastic fiber formation by binding structural components, including tropoelastin, the soluble precursor of elastin, fibrillin-1, and cross-linking enzymes. The cross-linking of tropoelastin monomers, which are deposited on the microfibril scaffold, involves several members of the lysyl oxidase family and leads to elastic fiber maturation. Cross-linking is also a pivotal step for elastin insolubility, proteolytic resistance, and longevity.<sup>3</sup>

The metabolic turnover of elastin is slow, with a half-life comparable to human lifespan.<sup>4</sup> However, sun damage or simply aging leads to the degradation of elastic fibers. This process is mainly driven by elastolytic enzymes, such as metalloproteinases (MMPs) and elastases, which are secreted by dermal fibroblasts, eventually leading to modifications of skin mechanical properties. MMP-12, also known as human macrophage metalloelastase, is the most active protease in elastin degradation.<sup>5</sup>

During aging, skin undergoes progressive, structural, and functional degeneration, leading to a reduced recoil ability whereas its relative stiffness significantly increases. Additionally, skin thickness inversely correlates with skin stiffness.<sup>6</sup> In vivo, loss of skin elasticity has been demonstrated to correlate with wrinkle severity, cheek sagging, and nasolabial fold formation. Besides, gravity tends to worsen skin sagging and ptosis of the lower part of the face. The combination of gravity and age-related loss of elasticity thus enhances the visible signs of aging.<sup>7</sup>

Using label-free proteomic analysis, we previously discovered that a NaLTTM (Natural Low-Transition Temperature Mixture) extract of *Murraya koenigii* leafy stems obtained with the tertiary solvent mixture betaine-water-propanediol (1:5:1 molar ratio) (BWP151) had a potential to regulate ECM remodeling and more specifically elastic fiber neogenesis (paper under peer review). In the present study, we further explored the elastogenic potential of such an extract at both in vitro and in vivo levels. For this, we measured both synthesis of different elastic fiber-related proteins and in vitro skin elasticity in a 3D microtissue models treated with *Murraya*

*koenigii* extract. We also conducted in vivo evaluation focusing on gravity-related parameters on healthy human volunteers.

## 2 | MATERIALS AND METHODS

### 2.1 | Pre-clinical evaluation

#### 2.1.1 | BWP151 extract of *Murraya koenigii*

Fresh leafy stems of *Murraya koenigii* were collected in June 2016 from La Réunion Island, and then immediately air-dried and ground to a fine powder. Before being processed, the sample was confirmed to be *Murraya koenigii* through DNA barcoding (DNA Gensee, Le Bourget du Lac, France).

Ground *Murraya koenigii* leafy stems were extracted using a mixture of betaine, water, and propanediol in a 1:5:1 molar ratio as solvent. This combination belongs to the NaLTTM family of solvents, which display well-described characteristics.<sup>8</sup> The solvent mixture is referred to as BWP151 hereinafter. The extract obtained in BWP151 may further be referred to as simply “the extract” in the following text. The phytochemical composition of the extract is characterized by a high content of polyphenols, mainly phenolic acids (0.45 g/Kg) and flavonoids (0.26 g/Kg) and the particularity of only trace of alkaloids (RP-HPLC-UV analysis).

#### 2.1.2 | 3D model of skin equivalent

*Fibroblasts* from juvenile foreskin (<2 years old) were seeded onto Alvetex® porous polystyrene scaffold inserts (AMSBIO, Abingdon, UK) and cultured for 4 weeks in CnT Prime fibroblast medium (CELLnTEC, Bern, Switzerland), supplemented with 50 µg.mL<sup>-1</sup> ascorbic acid (Sigma-Aldrich, Saint-Quentin Fallavier, France) and 10 ng.mL<sup>-1</sup> EGF (AMS Bio) at 37°C in a 5% CO<sub>2</sub>. Then, keratinocytes from juvenile foreskin (<2 years old) were seeded on top of the dermal equivalent and cultured in CnT Prime medium (CELLnTEC) for 3 days. The system was lifted at the air-liquid interface, and the culture was grown in CnT Prime Airlift medium (CELLnTEC) for 3 weeks. The quality of the underlying dermal equivalent permits the development of a multistratified epidermis. The reconstructed skin samples were treated with BWP151 extract of *Murraya koenigii* dissolved in the culture medium (0.1%) during the maturation of the dermis for 2 weeks, from day 14 until day 28, and during epidermal keratinization for two additional weeks, from day 35 until day 49.<sup>9</sup> Fresh extract was added every 2 days. Untreated samples were used as controls.

#### 2.1.3 | 3D scaffold-free model of spheroid microtissue

Adult fibroblasts were seeded in Ultra Low Affinity plates (In Sphero, Schlieren, Switzerland) and cultured in Fibroblast Growth Medium

1 (Promocell, Heidelberg, Germany) for 12 days. Spheroid microtissues were treated with BWP151 extract of *Murraya koenigii* dissolved in the culture medium (0.1%) during the last 4 days of culture. Untreated samples were used as controls.

## 2.1.4 | Immunofluorescence analysis

Primary antibodies were directed against human elastin (rabbit polyclonal antibody, reference 25011, Novotec, France), human fibrillin-1 (rabbit polyclonal antibody, Sigma-Aldrich, reference HPA021057, France), and human fibulin-5 (mouse monoclonal antibody, clone 1G6A4, Abcam, UK). Goat anti-rabbit Alexa Fluor 594 (Invitrogen, Carlsbad, CA, USA) and goat anti-mouse Alexa Fluor 594 (Invitrogen) were used as conjugates.

Samples of skin equivalent and spheroid microtissues were embedded in Tissue Tek OCT compound (Microm Microtech, Francheville, France), frozen in liquid nitrogen and cut to 5  $\mu$ m thick sections (Cryostat type HM 560, Microm Microtech, Francheville, France). The mounting medium (Prolong Gold antifade reagent, Thermo Fisher Scientific, Waltham, Massachusetts, USA) contained DAPI for nucleus staining. Fluorescent staining was observed using an Axio Imager M2 fluorescence microscope (Zeiss, Oberkochen, Germany) and quantified (area of ROI) using Zen image analysis software (Zeiss). Three independent experiments were performed in triplicate ( $n=3$ ).

Results were expressed as percentage of protein expression in *Murraya koenigii* treated cultures versus untreated ones (skin equivalents only). Data were expressed as means  $\pm$  standard deviations (SD). Statistical significance was assessed using nonparametric Wilcoxon rank-sum test.

## 2.1.5 | Two-photon autofluorescence microscopy

Whole fresh spheroid microtissues were analyzed under LSM880 confocal microscope (Zeiss) equipped with a "C-Apochromat" 40x/1.1M27 objective. Elastin autofluorescence was detected at exc. 890 nm/em. 445 nm and quantified (mean intensity of fluorescence) using ImageJ analysis software. Three independent experiments were performed in triplicate ( $n=3$ ). Results were expressed as percentage of elastin expression in extract-treated spheroid microtissues versus untreated spheroid microtissues. Data were expressed as mean  $\pm$  standard deviation (SD). Statistical significance was assessed using the nonparametric Wilcoxon test.

## 2.1.6 | Atomic force microscopy (AFM)

Both whole fresh spheroid microtissues and 20  $\mu$ m thick sections were analyzed under the AFM-Bioscope Resolve® (Bruker, Billerica, Massachusetts, USA) equipped with a DMI8 microscope (Leica, Wetzlar, Germany) to precisely position the AFM probe at the

center of the tissue. Two thousand points (10 spheroids analyzed with 200 force curves realized per spheroid) of measurement were captured to calculate Young's modulus using BioMeca analysis software (BioMeca®, Lyon, France). Three independent experiments were performed in triplicate ( $n=3$ ). Results were expressed as apparent stiffness (kPa) of *Murraya koenigii*-treated spheroid microtissue versus untreated spheroid microtissue. Distribution of data was expressed in box and whisker plots. The lower and the upper boundaries of the box represent the 25th and 75th percentiles of the data, respectively. The cross symbol inside the box represents the mean, and error bars show minimum and maximum nonextreme values. Statistical significance was assessed using the nonparametric Mann-Whitney test.

## 2.2 | Clinical evaluation

### 2.2.1 | Study design

A monocentric, double-blind study was performed under dermatological control to evaluate the antisagging potential of BWP151 extract of *Murraya koenigii*, which was formulated at 1% in an o/w emulsion (Table 1). Forty-five volunteers showing signs of aging and sagging in the lower part of the face and complying with the inclusion and exclusion criteria were enrolled in this study. Inclusion into the study required written informed consent, in accordance with the Declaration of Helsinki, and compliance with the following inclusion criteria: Caucasian women, aged 45–70, with all skin types and

TABLE 1 Formulations used in the clinical trial.

INCI	% Material
Water	76.15
Acrylates/C10-30 alkyl acrylate crosspolymer	0.10
Xanthan gum	0.30
Glycerin	4.00
Cetyl alcohol, glyceryl stearate, PEG-75 stearate, ceteth-20, and steareth-20	4.00
Cetearyl alcohol	2.00
Caprylic/capric triglyceride	4.00
Coco-caprylate	4.00
Isostearyl isostearate	3.00
Phenoxyethanol and ethylhexylglycerin	1.00
Water and sodiumhydroxide	0.25
Betaine, water, propanediol, and <i>Murraya koenigii</i> stem extract	<b>1.00</b>
Parfum	0.20
<b>100.00</b>	

Note: BWP151 *Murraya koenigii* stem extract was replaced by water in the placebo formula.

Bold value is *Murraya Koenigii* extract and its solvent used for in vitro objectification assays contained at 1% in the formula.

Fitzpatrick skin phototypes I–III, having a body mass index (BMI) of 20–28, with stable hormonal status (no pregnancy, no nursing, no change in hormonal contraception, no menopause, and no change in hormonal replacement therapy, if any, during the past 6 months) having visible clinical signs of aging and sagging on the lower part of the face as assessed by a trained beautician, by clinical scoring of two main criteria: ptosis or sagging of the oval of the face and depth of the nasogenian folds, both with a minimum grade of 3 according to the Skin Aging atlas of Bazin et al.<sup>10</sup> Exclusion criteria were the presence of any skin pathologies and skin abnormalities, a history of allergies or hypersensitivity to the test product, acute and/or chronic diseases and/or topical or systemic treatment assessed to be unsuitable for the enrollment of the volunteer by the investigator dermatologist, pregnancy and breastfeeding, a history of laser treatment or mesotherapy or product injections to the face in the previous 6 months, an exposure to sunlight or artificial UV rays within 1 month.

The study was carried out in France from January 27, 2020 to May 7, 2020. According to French law, the study should not be considered a research study and thus did not require any specific authorization. The test product was applied for 98 days twice a day (in the morning and in the evening) on the whole face on clean and dry skin with slight massages until complete penetration. The first application of the test product was performed at day 0 at the laboratory under the control of a beautician, then the test product was applied in normal conditions of use by the volunteers themselves at home. The last application of the product was made at day 97 in the evening. Volunteers were asked not to change their daily habits, to avoid sun exposure and to only use the test product for their skin care routine. The compliance of volunteers with the product application was assessed by weighing the test product before the first application at day 0, and at day 98, after 98 days of repeated applications. Additionally, volunteers were asked to complete a daily log during the study indicating the number of applications per day completed and any comments or observations. Evaluations were performed at day 0 before the first application and at day 98 after 98 days of repeated applications.

### 2.2.2 | Clinical scoring of the gravity impact

The severity of nasogenian folds and jowls was evaluated by a trained beautician in both sitting and supine positions through a visual sensory evaluation using a 5-point scale (from 1 to 5, with intermediate grades of 0.5 authorized) under standardized, controlled environmental conditions (temperature and hygrometry). For the sitting position, volunteers had to sit upright, eyes staring at the horizon, on an EvaLux Bench® (Orion Concept, Tours, France). For the supine position, volunteers laid down on an examination bed. Then, the severity scores of nasogenian folds and jowls were added up to obtain the global gravity score. Assessments were carried out under controlled environmental conditions ( $22 \pm 2^\circ\text{C}$ , HR  $45 \pm 5\%$ ).

### 2.2.3 | AEVA-HE measurements and image analysis

AEVA-HE (Eo TechSA) uses a patented fringe-projection unit combined with stereo imaging techniques to obtain 3D acquisitions. Subsequent image analyses were performed by Newton Technologies (Lyon, France). Morphological parameters of nasogenian folds were determined as described previously.<sup>11</sup> Analyses were performed on one half of the face.

### 2.2.4 | Illustrative pictures

Pictures were taken at baseline (D0) in supine and sitting positions, then in sitting position after 98 days of treatment. An arm device mounted on an examination bench was designed to hold a camera (Nikon 5200) above the face of volunteers, thus allowing to capture images in lying position (Laboratoire BIO-EC).

## 3 | RESULTS

### 3.1 | BWP151 extract of *Murraya koenigii* improved the deposition of elastin and fibrillin-1 in a 3D skin-equivalent model

Using a full-thickness skin-equivalent model, we evaluated the ability of BWP151 *Murraya koenigii* extract to improve the protein expression and deposition of elastin and fibrillin-1, both of which are key components of elastic fibers. The extract was added at 0.1% to the culture medium during dermal maturation and epithelialization. Skin models were kept in culture for 49 days, to obtain a mature dermal equivalent that favors the development of a well-organized, stratified, and terminally differentiated epidermis (Figure 1A). When grown in the presence of the extract, the overall architecture of reconstructed skin was similar to that of untreated cultures (Figure 1B). Likewise, immunostainings revealed increased protein expression and deposition of both elastin ( $+145\% \pm 101$ ;  $p < 0.0001$ ) and fibrillin-1 ( $+71\% \pm 62$ ;  $p < 0.001$ ) (Figure 1C–F).

### 3.2 | BWP151 extract of *Murraya koenigii* allowed for the synthesis of a structurally organized network of elastin deposits and endowed elastogenic properties in a 3D model of spheroid microtissue

To assess whether increased protein syntheses resulted in improved elasticity in vitro, a 3D model of spheroid microtissue in which we previously showed that mechanical and structural elastic properties were closely related<sup>12</sup> was grown in the presence of BWP151 extract of *Murraya koenigii*. Because functional elastic fibers are highly organized molecular structures, we looked at the

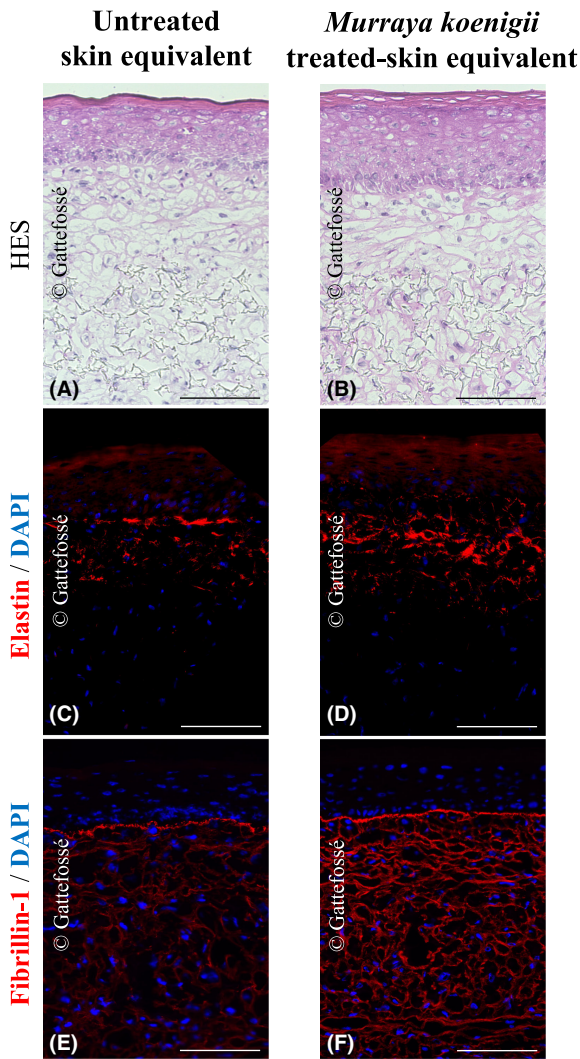


**FIGURE 1** BWP151 extract of *Murraya koenigii* improved synthesis and deposition of both elastin and fibrillin-1 in a 3D model of skin equivalent. (A,B) Hematoxylin-Eosin staining. (C–F) Immunostaining of elastin, fibrillin-1, and cell nuclei. Representative images of three independent experiments in triplicate ( $n=3$ ). Scale bar: 100  $\mu\text{m}$ .

macromolecular organization of elastin deposits in the spheroid microtissue. Using immunostaining of elastin and fibulin-5, we observed that both proteins were colocalized (Figure 2A–C,E), thus evidencing their proper macromolecular organization. Both proteins were also colocalized in spheroid microtissue treated for 4 days with the extract (Figure 2B–D,F). We used multiphoton microscopy to visualize the structural organization of the whole elastin deposits within the spheroid microtissue. Thanks to the two-photon autofluorescence of elastin, we showed that the extract enhanced (125%  $\pm$  77;  $p < 0.001$ ) the synthesis of an extensive elastin deposit network as compared to the untreated spheroid microtissue (Figure 2G,H).

As a functional approach, we then used AFM to measure the biomechanical properties of spheroid microtissues. Untreated samples had an apparent stiffness of around 40 kPa (Figure 3A),

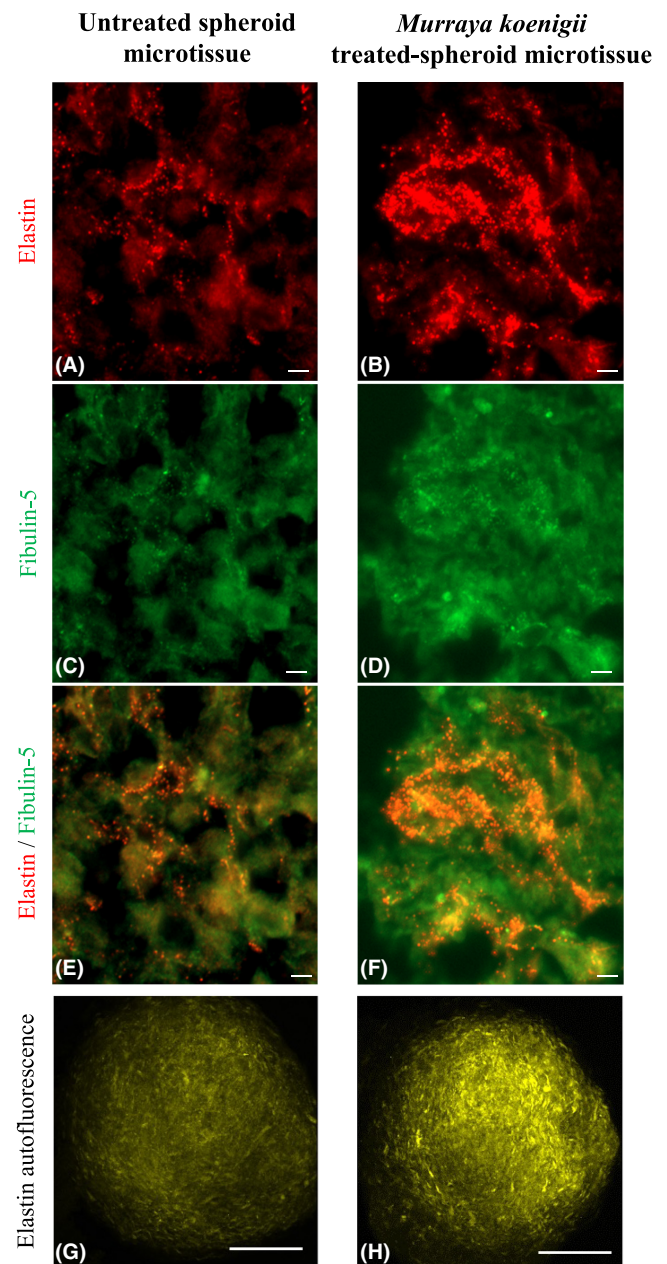


**FIGURE 2** BWP151 extract of *Murraya koenigii* induced the synthesis of a structurally organized network of elastin deposits in a 3D model of spheroid microtissue. (A–F) Immunofluorescence staining of elastin and fibulin-5. Scale bar: 5  $\mu\text{m}$ . (G–H): Two-photon autofluorescence of elastin (exc. 890 nm/em. 445 nm) taken from spheroid microtissues. Representative images of three independent experiments in triplicate ( $n=3$ ). Scale bar: 100  $\mu\text{m}$ .

which is close to the values reported for human skin.<sup>13</sup> In the presence of the extract (4 days), we showed that spheroid microtissues exhibited a significant decrease (3-fold,  $p < 0.0001$ ) of their apparent stiffness (Figure 3A), evidencing an improvement of tissue elasticity. We confirmed that elastin-rich areas (Figure 3B) were less stiff (Figure 3C), supporting the hypothesis that the observed elastin deposits took part of a process of effective functional elastic fiber assembly.

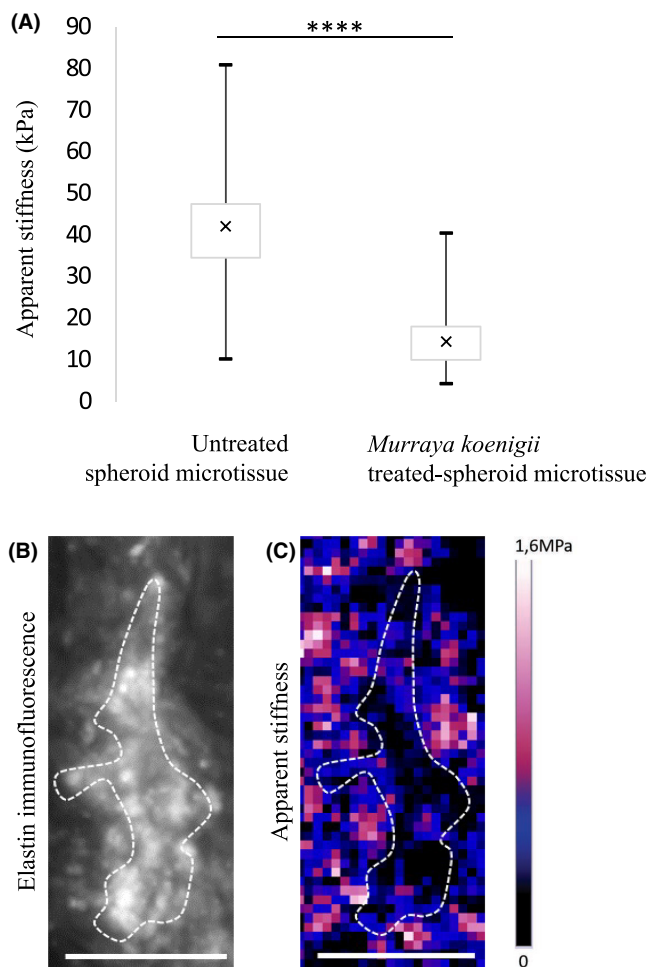


**FIGURE 3** BWP151 extract of *Murraya koenigii* induced the synthesis of a functional network of elastin deposits in a 3D model of spheroid microtissue. (A) Apparent stiffness (kPa) measured on whole spheroid microtissues using atomic force microscopy. \*\*\*\* $p$  value  $< 0.0001$  (Mann-Whitney test). (B,C) Combined analysis of elastin immunofluorescence and atomic force microscopy from spheroid microtissues. Elastin deposits are shown in white dots (B) and apparent stiffness is represented according to the gradient bar (C). Representative images of three independent experiments in triplicate ( $n = 3$ ). Scale bar: 30  $\mu\text{m}$ .

### 3.3 | BWP151 extract of *Murraya koenigii* visibly improved gravity-related signs of aging in vivo

Out of 45 volunteers enrolled, 37 completed the study without any major deviation (mean age:  $60.2 \pm 6.3$  years old, mean BMI:  $23.5 \pm 2.8$ ). No adverse reactions or events were reported.

For the nasogenian fold analysis from 3D acquisitions, the results were expressed for 21 volunteers, and not the 37 volunteers who completed the study. Indeed, 16 volunteers were removed from the analysis of the results because their 3D acquisitions could not be analyzed due to poor image quality (presence of artifacts) and/or due to a bad repositioning of the volunteers at day 98 compared to day 0, making analysis impossible.

When compared with D0, the total surface of nasogenian fold wrinkles was significantly reduced by 6.75% after 98 days of twice-daily application of a cosmetic emulsion containing the BWP151 *Murraya koenigii* extract at 1% ( $24.29 \pm 7.29$  vs.  $22.65 \pm 6.54$ ,  $p < 0.01$ , Student's  $t$ -test) (Figure 4). Likewise, the total length of nasogenian fold wrinkles was significantly reduced by 9.44% ( $61.84 \pm 21.28$  vs.  $56.00 \pm 16.42$ ,  $p < 0.01$ , Wilcoxon signed-rank test).

To evaluate the reduction of the impact of gravity over time, the clinical scores obtained in the supine position at D0 were used as a reference and compared to values obtained in the sitting position either at D0 (initial impact of gravity) or after 98 days of treatment (final impact of gravity) (Figure 5). To be noticed, results were expressed for the 37 volunteers who completed the study. At D0, in supine position, the mean clinical score for the severity of nasogenian folds was of  $2.86 \pm 0.62$ , compared to  $3.69 \pm 0.70$  in sitting position, which represented a 28.8% increase in the severity of nasogenian folds when changing from a low gravity position (supine) to a high gravity position (sitting) ( $p < 0.0001$ , Wilcoxon signed-rank test). After 98 days of treatment, the mean clinical score in sitting position was of  $3.15 \pm 0.96$ , which represented a 9.9% increase in the visibility of nasogenian folds when switching virtually from baseline supine position (D0) to sitting position at D98 ( $p < 0.01$ , Wilcoxon signed-rank test). In other words, the impact of gravity on the severity nasogenian folds was reduced by two-third after 98 days of treatment with the extract (Table 2).

Likewise, in supine position, the mean clinical score of jowl severity at D0 was of  $2.84 \pm 0.51$  compared to  $3.85 \pm 0.50$  in sitting position which represented a 35.7% increase in the severity of jowls when changing from a low gravity position (supine) to a high gravity position (sitting) ( $p < 0.0001$ , Wilcoxon signed-rank test). After 98 days of treatment, the mean clinical score in sitting position was of  $3.49 \pm 0.62$ , which represented a 22.9% increase in the severity of jowls ( $p < 0.0001$ , Wilcoxon signed-rank test). The impact of gravity on the severity of jowls was thus virtually reduced by one-third after 98 days of treatment with the extract.

When calculating the global score of gravity (severity nasogenian folds + jowls), scores obtained were of  $5.70 \pm 1.04$  at D0 in supine position,  $7.54 \pm 1.07$  at D0 in sitting position, and of  $6.64 \pm 1.39$  in sitting position after 98 days of treatment with *Murraya koenigii* extract. Thus, when comparing data obtained at D0, the transition from supine to sitting position triggered a 32.2% increase in gravity scores ( $p < 0.0001$ , Student's  $t$ -test). This increase was virtually only 16.4% ( $p < 0.0001$ , Student's  $t$ -test) when comparing the gravity score in the supine position at D0 to that in the sitting position at D98. In other words, after 98 days, the cosmetic formulation containing 1% of the extract allowed to significantly reduce the impact of gravity of facial traits.

## 4 | DISCUSSION

Facial traits of skin aging include a loss of elasticity, which is accompanied by the formation of wrinkles, a sagging of the lower part of the

**FIGURE 4** Image analysis of nasogenian fold wrinkles. Illustrative example of a 48-year-old volunteer at baseline (D0) and after 98 days of treatment: 2D projected picture (left) and 2D projected picture with last segmentation (right) for each time-point.

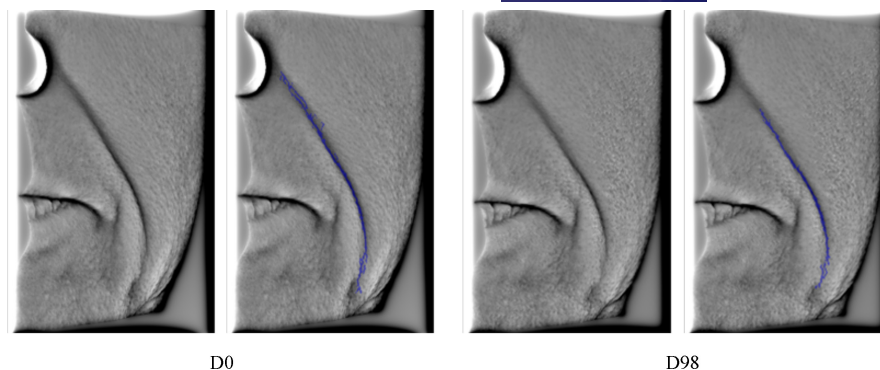


**FIGURE 5** Illustrative pictures of the impact of gravity on facial traits. Illustrative example of a 51-year-old volunteer before and after 98 days of treatment. Compared to baseline, the severity of facial traits (nasogenian folds and jowls) in sitting position was reduced.

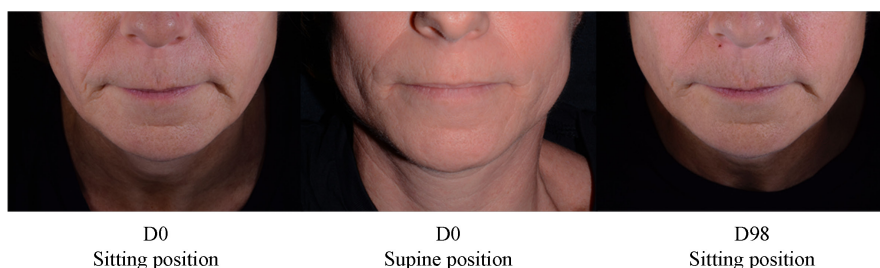


**TABLE 2** Clinical scoring of the impact of gravity.

Emulsion containing 1% of BWP151 extract of <i>Murraya koenigii</i>	Clinical scoring in vivo (mean scores $\pm$ SD)		
	D0. Sitting position	D0. Supine position	D98. Sitting position
Severity of nasogenianfolds	3.69 $\pm$ 0.70	2.86 $\pm$ 0.62	3.15 $\pm$ 0.96
% of variation vs. D0 supine position	+28.8%****	-	+9.9%**
Severity of jowls	3.85 $\pm$ 0.50	2.84 $\pm$ 0.51	3.49 $\pm$ 0.62
% of variation vs. D0 supine position	+35.7%****	-	+22.9%****
Global score: (Severity of nasogenianfolds + jowls)	7.54 $\pm$ 1.07	5.70 $\pm$ 1.04	6.64 $\pm$ 1.39
% of variation vs. D0 supine position	+32.2%****	-	+16.4%****

Note: Severity scores of nasogenian folds and jowls are added up to obtain the global gravity score. Statistical significance was assessed using Student's t-test or Wilcoxon signed-rank test: \*\* $p < 0.01$ ; \*\*\*\* $p < 0.0001$ .

face and loss in the harmony of facial contours. Ultrastructural, morphometric, and mechanical studies have demonstrated that major alterations in aged skin occur in the dermal ECM,<sup>14</sup> especially at the level of the elastic fiber network. Due to their long half-life, elastic fibers accumulate damage during aging, ultimately leading to their degradation and loss of functionality. The formation and maturation of elastic fibers encompass a complex multistage process called elastogenesis. It requires interactions between several structural proteins and partners to allow for the deposition and cross-linking of tropoelastin, on a scaffold of fibrillin-rich microfibrils, a prerequisite for elastic fiber functionality. Indeed, fibrillin microfibrils serve as structural scaffold required for tropoelastin alignment, and particularly fibrillin-1 is believed to promote coacervation of tropoelastin into larger and dense globules.<sup>15</sup> An elastic fiber is described as "mature" when tropoelastin monomers form a durable and insoluble biopolymer through the aggregation of their hydrophobic domains,

their deposition onto a scaffold of fibrillin-rich microfibrils, and finally the involvement of various types of inter- and intra-molecular crosslinks by the action, among others, of members of the lysyl oxidase family.<sup>16</sup>

Using proteomic data on monolayer cultures of normal human fibroblasts, we previously identified a novel extract of *Murraya koenigii* leafy stems obtained using a mixture of betaine, water, and propane-1,2-diol as extraction solvent with promising ECM-boosting properties (paper under review). The extract is characterized by a high content of both flavonoids and phenolic acids and a very low content in alkaloids, which are often reported to bear the biological activities of *Murraya koenigii* herbal remedies.<sup>17</sup> To dig deeper into the biological properties of the BWP151 *M. koenigii* extract, the synthesis of elastic fiber-related proteins was further evaluated in monolayer cultures of adult fibroblasts of different ages (18 and 50 years old) (S1). Interestingly, the extract at 0.1% significantly increase the

expression and in situ deposition of elastin ( $+43\% \pm 19$ ,  $p < 0.0001$ ), fibrillin-1 ( $+22\% \pm 29$ ,  $p < 0.05$ ), and fibulin-5 ( $+62\% \pm 13$ ,  $p < 0.05$ ). However, monolayer cultures of fibroblasts do not integrate the complexity of cell-cell and cell-matrix interactions of the naturally occurring 3D environment, and thus offer limited predictability of in vivo benefits. Indeed, it has been shown that the 3D environment significantly influence the morphology, phenotype, and metabolic activity of fibroblasts in culture.<sup>18</sup> More specifically, in vitro elastogenesis has been shown to be significantly improved in the presence of epidermal keratinocytes.<sup>19,20</sup> We thus decided to use full-thickness skin models to confirm the previously observed ability of the BWP151 *M. koenigii* extract at boosting elastic fiber-related proteins.

In our study, the extract improved the syntheses of both elastin ( $+145\% \pm 101$ ;  $p < 0.0001$ ) and fibrillin-1 ( $+71\% \pm 62$ ;  $p < 0.001$ ) in a 3D engineered skin model.

Besides, we also studied the ability of the extract to prevent proteolytic degradation of elastic fibers in vitro. Many matrix metalloproteinases (MMPs) degrade elastic fibers but MMP-12 is the most active protease in elastin degradation as it is reported to have at least 86 cleavage sites in the tropoelastin protein. Interestingly, the proteolytic activity of MMP-12 was significantly and dose-dependently decreased (from 0.05% to 0.5%) in monolayer cultures of fibroblasts treated with the extract for 48h (S2).

Beyond structural aspects, elastic fiber functionality, meaning their extensibility and resilience, is key to skin biomechanical properties. Therefore, we considered that measuring the elastic properties in vitro was a necessary step to confirm that increased syntheses of elastic fiber-related proteins effectively resulted in improved dermal biomechanical properties. However, most of 3D skin models use biomaterials as a scaffold to recreate a frame necessary for the adhesion of fibroblasts before ECM synthesis and organization.<sup>21</sup> Those scaffolds create artifacts when measuring skin mechanical properties and dermal elasticity.<sup>22</sup> Therefore, we used a scaffold-free in vitro model of spheroid microtissue, whose mechanical properties correlate with elastogenic potential to investigate the efficacy of the extract on skin elastic properties.<sup>12</sup> In that model, the extract allowed for the synthesis of macromolecular structures in which elastin and fibulin-5 were properly colocalized. In addition, using multiphoton microscopy, intense two-photon autofluorescence of elastin was detected, thus confirming the ordered macrostructure of elastin deposits within microtissues treated with the extract.

Atomic force microscopy was used in parallel to measure dermal stiffness in vitro. We observed that the extract improved tissue elasticity as measured by a 3-fold decrease in the apparent stiffness of microtissue with a Young's modulus of 15kPa, consistent with the values of Young's Modulus reported to usually range from 5 to 100kPa based on indentation methods.<sup>23</sup> Furthermore, combined analysis of elastin immunostaining and atomic force microscopy allowed to draw a correlation map of apparent stiffness and elastin deposit density, which revealed that elastin-rich areas were less stiff. In other words, this study evidenced a good correlation between the increased amount of elastin-containing macromolecular structures and their functionality further to the treatment of the extract.

Backed by promising in vitro results obtained in 2D and 3D models, we decided to further evaluate the clinical benefits of the extract. Nasogenian folds are part of those facial traits particularly affected by gravity, loss of elasticity, and eventually, skin sagging.<sup>24</sup> We first used fringe-projection combined with image analysis to measure the severity of nasogenian folds. When compared with D0, both the surface and length of nasogenian fold wrinkles were significantly reduced by 6.75% and 9.44%, respectively ( $p < 0.01$ ) at D98. The impact of gravity on the visible signs of aging around the eyes and in the lower part of the face was studied on volunteers placed in sitting position and compared to supine position. Indeed, in supine position, the impact of gravity is considered to be the lowest, with reduced depth of the tear trough, blurred eye bags, nasogenian folds less visible and restored volume of the cheeks.<sup>24</sup> To assess the evolution of the impact of gravity, we thus used the supine position at D0 as reference and compared the data obtained in sitting position at D0 and after 98 days of product application. A global score of gravity, which combined the clinical evaluations of nasogenian folds severity and jowls severity was calculated in the different positions at the different measurement timepoints. After 98 days of treatment, the difference in global gravity scores between supine and sitting positions was significantly reduced from 32.2% to 16.4% ( $p < 0.0001$ ). In other words, when used at 1% in a cosmetic formulation, the extract allowed to visibly reduce the impact of gravity of facial traits. All the clinical data obtained revealed the usefulness of this extract formulated at 1% to visibly reduce nasogenian fold severity, jowl severity and to mitigate the impact of gravity on the facial signs of aging after 98 days of repeated applications and is expected to be an effective cosmetic aid in reducing facial signs of aging.

Taken together, our in vitro and in vivo data highlight that the newly discovered BWP151 extract of *Murraya koenigii* leafy stems represents an innovative antiaging ingredient particularly suited for elasticity-boosting and antisagging claims.

## AUTHOR CONTRIBUTIONS

S. Bonnet and A. Lopez-Gaydon performed the experiments. C. Lorion, V. Bardin, N. Bechetoille, and B. Vogelgesang provided the idea and designed the experiments. C. Lorion and V. Bardin wrote the paper.

## ACKNOWLEDGMENTS

We are grateful to BioMeca for their technical contribution and assistance to SHG/AFM analyses. We thank Laboratoire BIO-EC for their assistance in conducting the clinical study at their facilities and for the assessment of the impact of gravity on volunteers' facial traits. We also thank Newton Technologies for their assistance in the image analysis of fringe-projection data of nasogenian folds.

## FUNDING INFORMATION

This study was totally funded by Gattefossé SAS.

## CONFLICT OF INTEREST STATEMENT

The authors have no conflicts of interest to declare.

## DATA AVAILABILITY STATEMENT

The data that support the findings of this study are available from the corresponding author upon reasonable request.

## ETHICS STATEMENT

Authors declare human ethics approval was not needed for this study.

## ORCID

Chloé Lorion  <https://orcid.org/0009-0009-3372-0657>

Nicolas Bechetoille  <https://orcid.org/0000-0001-5260-3469>

## REFERENCES

- Muiznieks LD, Weiss AS, Keeley FW. Structural disorder and dynamics of elastin. *Biochem cell biol.* 2010;88:239-250.
- Kielty CM, Sherratt M, Marson A, Baldock C. Fibrillin Microfibrils. *Fibrous Proteins: Coiled-Coils, Collagen and Elastomers (Advances in Protein Chemistry)*. Elsevier; 2005:405-436.
- Kielty CM, Baldock C, Lee D, Rock MJ, Ashworth JL, Shuttleworth CA. Philosophical transactions of the Royal Society of London. Series B, Biological Sciences. *Philos Trans R Soc Lond B Biol Sci.* 2002;357:207-217.
- Uitto J, Paul JL, Brockley K, Pearce RH, Clark JG. Elastic fibers in human skin: quantitation of elastic fibers by computerized digital image analyses and determination of elastin by radioimmunoassay of desmosine. *Lab Invest; a Journal of Technical Methods and Pathology.* 1983;49:499-505.
- Lamort A-S, Gravier R, Laffitte A, Juliano L, Zani M-L, Moreau T. New insights into the substrate specificity of macrophage elastase MMP-12. *Biol Chem.* 2016;397:469-484.
- Kalra A, Lowe A. An overview of factors affecting the skins Youngs modulus. *J Aging Sci.* 2016;4:1-5.
- Park JW, Lee M, Kim J, Kim E. Quantitative evaluation of facial sagging in different body postures using a three-dimensional imaging technique. *J Cosmet Dermatol.* 2020;20:2583-2592.
- Francisco M, van den Bruinhorst A, Kroon MC. Low-transition-temperature mixtures (LTTMs): a new generation of designer solvents. *Angew Chem Int Ed Engl.* 2013;52:3074-3085.
- Auxenfans C, Fradette J, Lequeux C, et al. Evolution of three dimensional skin equivalent models reconstructed in vitro by tissue engineering. *Eur J Dermatol.* 2009;19:107-113.
- Bazin RDE. Paris: Editions Med'Com. 2007.
- Campiche R, Trevisan S, Sérout P, et al. Appearance of aging signs in differently pigmented facial skin by a novel imaging system. *J Cosmet Dermatol.* 2019;18:614-627.
- Lorion C, Lopez-Gaydon A, Bonnet S, Drillat A, Milani P, Bechetoille N. 619 Structural and biomechanical properties of a novel 3D microdermis model: the spheroid. *J Invest Dermatol.* 2019;139:S321.
- Pailler-Mattei C, Bec S, Zahouani H. In vivo measurements of the elastic mechanical properties of human skin by indentation tests. *Med Eng Phys.* 2008;30:599-606.
- Fisher GJ, Varani J, Voorhees JJ. Looking older: fibroblast collapse and therapeutic implications. *Arch Dermatol.* 2008;144:666-672.
- Adamo CS, Zuk AV, Sengle G. The fibrillin microfibril/elastic fibre network: A critical extracellular supramolecular scaffold to balance skin homeostasis. *Exp dermatol.* 2020;30:25-37.
- Schmelzer CEH, Duca L. Elastic fibers: formation, function, and fate during aging and disease. *FEBS J.* 2022;289:3704-3730.
- Nagappan T, Segaran T, Wahid M, Ramasamy P, Vairappan C. Efficacy of Carbazole alkaloids, essential oil and extract of *Murraya koenigii* in enhancing subcutaneous wound healing in rats. *Molecules.* 2012;17:14449-14463.
- Grinnell F. Fibroblast biology in three-dimensional collagen matrices. *Trends Cell Biol.* 2003;13:264-269.
- Duplan-Perratt F, Damour O, Montrocher C, et al. Keratinocytes influence the maturation and Organization of the Elastin Network in a skin Equivalent11The authors declared in writing to have no conflict of interest. *J Invest Dermatol.* 2000;114:365-370.
- Aya R, Ishiko T, Noda K, et al. Regeneration of elastic fibers by three-dimensional culture on a collagen scaffold and the addition of latent TGF- $\beta$  binding protein 4 to improve elastic matrix deposition. *Biomaterials.* 2015;72:29-37.
- Nikolova MP, Chavali MS. Recent advances in biomaterials for 3D scaffolds: a review. *Bioact Mater.* 2019;4:271-292.
- Tupin S, Molimard J, Cenizo V, Hoc T, Sohm B, Zahouani H. Multiscale approach to characterize mechanical properties of tissue engineered skin. *Ann Biomed Eng.* 2016;44:2851-2862.
- Alexander H, Cook TH. Accounting for NATURAL tension in the mechanical testing of human skin. *J Invest Dermatol.* 1977;69:310-314.
- Flament F, Bazin R, Piot B. Influence of gravity upon some facial signs. *Int J Cosmet Sci.* 2015;37:291-297.

## SUPPORTING INFORMATION

Additional supporting information can be found online in the Supporting Information section at the end of this article.

**How to cite this article:** Lorion C, Bardin V, Bonnet S, Lopez-Gaydon A, Vogelgesang B, Bechetoille N. Elastogenic potential and antisagging properties of a novel *Murraya koenigii* extract. *J Cosmet Dermatol.* 2023;00:1-9. doi:[10.1111/jocd.16059](https://doi.org/10.1111/jocd.16059)